(iÐiii) and their reßection in the switch in orbital texture

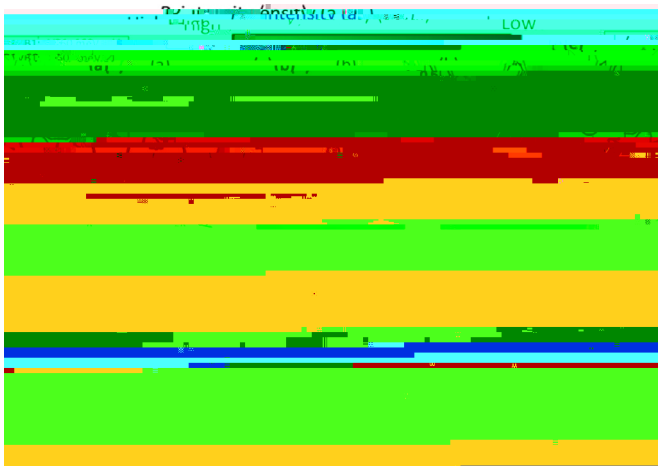

FIG. 2. (a–d) Orbital texture indicated by

VI. UNDERSTANDING THE SPIN-POLARIZATION EFFECTS

Equations (3) and (4) show that each orbital component couples with a certain spin state, forming orbital-dependent spin textures [see Eq. (2)]. Maximal spin magnitude arises when every orbital-dependent spin texture coaligns, i.e., has the same helicity. This requires that the band eigenstate be composed exclusively of orbitals with the same azimuthal quantum number m_l. In real materials where SOC mixes orbitals with different m_l in one eigenstate $n(\mathbf{k})$, the corresponding spin polarization is truncated relative to its maximal value. Specifically, the tangential in-plane orbital (p_t) always couples opposite spin texture to that of radial in-plane orbital (p_r), s, and p_z orbital. At the wave vector $\mathbf{K}$ with $k = 0$, p_t and p_r components have the same intensity but opposite spin pattern and thus cancel each other, making the spin polarization $S(k = 0) = |\ _{VB}|^2$ all contributed by the s and p_z orbitals. This scenario gives the truncated spin polarization at $\mathbf{K}$ for all the bands shown in Fig. 1(c). The total spin polarization summing over all bands is equivalent to the value obtained from the contributions of $m_l = 0$ states, e.g., s, p_z, and d_z^2, etc. This statement is valid also in the traditional 2D Rashba systems such as Au(111) surface [11], in which the surface Rashba bands are nearly exclusively composed by the s and p_z states, and thus have nearly 100% spin polarization.

Due to the orbital texture switch, we find from Eqs. (3) and (4) that the dominate in-plane p orbitals of a pair of Rashba bands couple to spin textures with the same helicity. This fact is confirmed by DFT calculation showing that the dominating radial orbital for VB1 and tangential orbital for VB2 both have RH spin texture (see Fig. 4). In BiTeI, the wave functions of VB1 and VB2 are dominated by $s + p_z$ orbitals [Te-p_z (50%), I Š p_z (13%), and Bi-s (13%)]. We consider here two categories of orbitals classified by $m_l = 0$ (s and p_z for all sites) and $m_l = 1$ (in-plane p_x and p_y for all sites) and examine the corresponding spin textures coupled by these two classes. The $s + p_z$-dependent spin texture has opposite helicity for VB1 and VB2; i.e., VB1 has a right-handed (RH) spin texture, while VB2 has a left-handed (LH) spin texture (see Fig. 5). On the other hand, the in-plane orbital ($p_x + p_y$) also contributes helical spin textures, but these orbital-dependent spin textures have the same RH helicity for both VB1 and VB2, as shown by the white arrows in Figs. 4(a) and 4(b). This can also be understood by multiorbital model equations (1) and (2), where the p_r (p_t) orbitals always provide positive (negative) contributions to the $s + p_z$-orbital-dependent spin textures. Consequently, at a k with the different intensity of p_t and p_r orbitals for VB1 and VB2 can cause different spin magnitudes to the respective bands, and thus a nonzero net spin polarization S

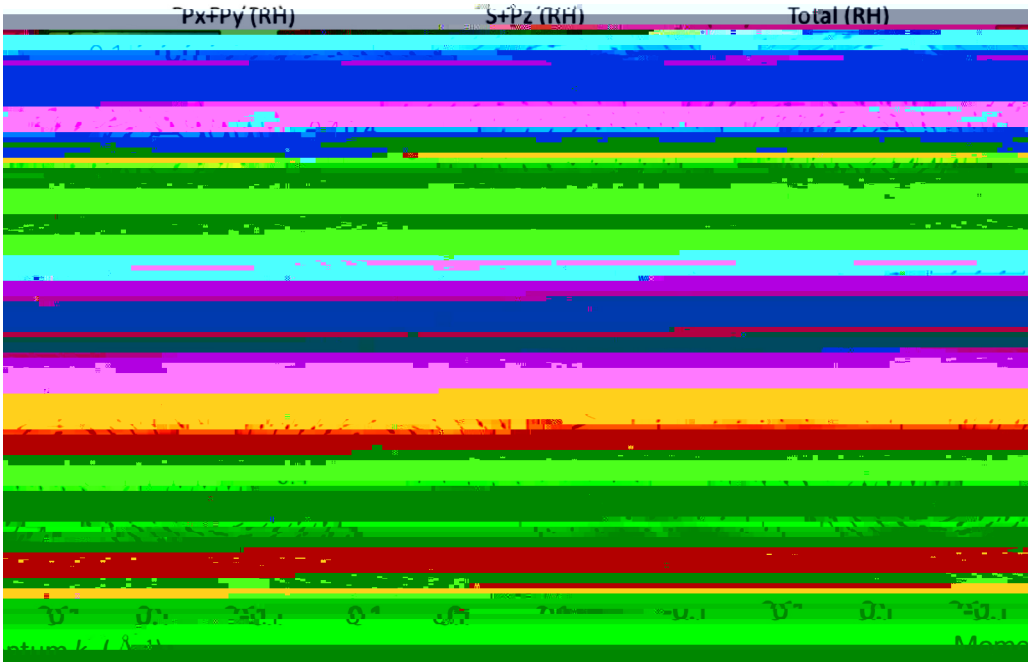

FIG. 5. Orbital-dependent spin texture coupled by in-plane orbital ($p_x + p_y$) and $m_l = 0$ orbital ($s + p_z$), and the total spin texture of VB1 (upper row) and VB2 (lower row). The background color indicates the out-of-plane spin component S_z. Left-handed (right-handed) in-plane spin texture S_x (S_y).

VII. EFFECTS OF DIFFERENT SOC STRENGTH

To demonstrate that the intriguing spin-polarization effects originate from SOC we artificially rescaled the strength of SOC by adding a multiplier on the SOC Hamiltonian (= 1 for the real system). The spin magnitude and spin-splitting energy E_R

TABLE I. Direction of atomic-orbital-dependent spin textures in the vicinity of the X point. S_1 and S_2 form in-plane and perpendicular Bi-S bonds, respectively.

	s	p_x	p_y	p_z
Bi	+	+	−	+
S_1	−	−	+	−
S_2	+	+	−	+

We choose a centrosymmetric R-2 material, LaO_2BiS (using the reported space group $P4/nmm$), to illustrate the truncation effects. Figures 8(a) and 8(e) exhibit the projected atomic-orbital-dependent spin textures of LaO_2BiS on one BiS_2 layer of the twofold degenerated conduction band minimum (CBM) and valence band maximum (VBM), respectively. The local spin textures on the other BiS_2 layer are exactly oppositely formed [25], and are not shown here. All the spin textures are in the x-y plane, with almost zero z component. We observe helical spin for holes but nonhelical spin for electrons, suggesting Rashba-type polarization (R-2) and the combination of Rashba and Dresselhaus effects (R-2 and D-2) for VBM and CBM, respectively. In general, the environment of R-2 material contains simultaneously polar field and inversion asymmetry, indicating the coexistence of R-2 and D-2 effects, depending on different band characters.

We note that the hole spin is nearly fully polarized with the spin magnitude 90%, while the electron spin is only 30% polarized. Besides the spin mixture effect due to the interlayer coupling (vanished along the X-M direction), the reason that leads to the partial polarization is the diverse atomic-orbital-dependent spin textures. Figures 8(b)–8(d) and 8(f)–8(h) show the spin textures from different atomic orbitals within one BiS_2 layer. We see all the orbital-dependent spin textures are parallel or antiparallel to the total spin texture, and they can make either

[1] A. Manchon, H. C. Koo, J. Nitta, S. M. Frolov, and R. A. Duine, Nat. Mater. 14, 871 (2015).
[2] C. Ciccarelli, M. D. HalsKjetil, A. Irvine, V. Novak, Y. Tserkovnyak, H. Kurebayashi, A. Brataas, and A. Ferguson, Nat. Nanotechnol. 10,